Journal of Applied Polymer Science

Experimental investigation of moisture diffusion in short-glass-fiber-reinforced polyamide 6,6

Shi Zhang, Zhigao Huang, Yun Zhang, Huamin Zhou
State Key Laboratory of Material Processing and Die & Mold Technology, Huazhong University of Science and Technology, Wuhan, Hubei, China
Correspondence to: H. Zhou (E-mail: hmzhou@hust.edu.cn)

ABSTRACT: Moisture diffusion in polyamide 6,6 (PA66) and its short glass fiber-reinforced composites has a great influence on their mechanical properties and service lives under hydrothermal environments. Hence, the moisture diffusion in neat PA66 and its composites was studied comprehensively in this study with the general Fickian model. To systematically investigate the effects of the fiber content, humidity, temperature, and humidity–temperature coupling effect on the diffusion coefficient and equilibrium concentration, gravimetric experiments for the PA66 composites were carried out under different hydrothermal conditions. The results show that the equilibrium moisture concentration depended on the relative humidity and fiber content but only depended weakly on temperature. The diffusion velocity was affected by the three aforementioned factors with different trends. The analysis of variance demonstrated that the humidity–temperature coupling effect played an important role in the diffusion process. The regression analysis gave the corresponding quadratic regression equations. © 2015 Wiley Periodicals, Inc. J. Appl. Polym. Sci. **2015**, *132*, 42369.

KEYWORDS: aging; composites; molding; polyamides

Received 6 February 2015; accepted 14 April 2015
DOI: 10.1002/app.42369

INTRODUCTION

Short-glass-fiber-reinforced (SGFR) polyamide 6,6s (PA66s) are excellent composites and have been widely used in numerous engineering applications in terms of their desirable mechanical performance and thermal stability.[1] However, because of the polar amide groups, SGFR PA66s tend to absorb a high level of water when they are exposed to humid environments, and the absorbed water has a great influence on the mechanical properties.[2–6] The process of hydrothermal aging can usually be divided into two parts: moisture diffusion and the influence of a certain amount of absorbed water on the mechanical properties. The effect of quantitative water on the mechanical properties of reinforced PA66 has been studied widely. Thomason and Porteus[7] studied the swelling of reinforced PA66 caused by water. Hassan and coworkers[1,6] focused on the changes in the dynamic mechanical properties after water absorption. Miri *et al.*[5] investigated the effect of water on the plastic deformation behavior. Launay *et al.*[4] were interested in the variation of the time effects of viscoelastic fiber-reinforced PA66. Hence, a sophisticated understanding of moisture diffusion in PA66 composites under hydrothermal conditions is of great significance.

There have been several studies that focused on the underlying mechanism of moisture diffusion. The Flory–Huggins model,[8,9] ENSIC (engaged species induced clustering) model,[10] modified Park model,[11] and GAB (Guggenheim–Anderson–de Boer)model[12,13] were built gradually. Those physical-based models are microscopic and cannot directly guide waterproof design. Moisture ingression is an essential factor in determining the durability of PA66 composites. To predict the life span of PA66 composites, phenomenological macroscopic diffusion models are being pursued.

Generally, the macroscopic models of moisture diffusion can be divided into two categories: the Fickian model and non-Fickian models. The Fickian model is expressed as follows:[14]

$$\frac{\partial C}{\partial t} = \frac{\partial}{\partial x}\left(D\frac{\partial C}{\partial x}\right) \tag{1}$$

where C is the concentration of the diffusing substance, D is the diffusion coefficient denoting the velocity of diffusion, and x is the thickness direction. At a given concentration, D can be approximately regarded as a constant with respect to the dimensions and time.[14] Because of the Fickian law, the mass of absorbed water will reached an equilibrium plateau. This model has been adopted widely to study moisture diffusion in composites.[15,16] Non-Fickian or anomalous behavior may directly come from the influence of the changing substance structure on the solubility and diffusional mobility. Non-Fickian models

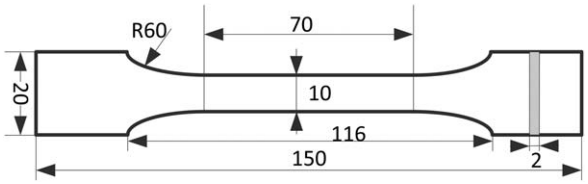

Figure 1. Sketch of the samples.

need more parameters than the Fickian model to describe the inherent interacting diffusion.[14]

In reality, most diffusion processes in polymer composites show more or less non-Fickian behaviors, especially for long exposure times. However, for a relatively short time, the diffusion process can generally be modeled by the Fickian law,[17] and it was also used for SGFR PA66s in this study.

For the Fickian model, D and the equilibrium concentration (C_∞) are its two key parameters. The effects of environmental factors on these two parameters are fundamental issues that attract researchers' attention. Temperature is an essential environmental factor affecting the diffusion process. The temperature dependence of D can be described well by the Arrhenius equation.[18,19] In contrast to D, the relation between C_∞ and temperature is still a controversial issue. C_∞ has been reported to be independent of temperature,[20,21] whereas either positive or negative temperature dependences have also been observed.[22,23] As for the fiber content in composites, it is considered to have an important influence on both D and C_∞.[24,25] Humidity as another critical environmental factor has also been taken into account. It is usually considered to have a positive influence on diffusion.[2,25,26] On the basis of a literature survey, it is known that environmental factors (including temperature, humidity, and fiber content) affect the parameters of the Fickian model. However, none of the open literature reports on mathematical models between these environmental factors and D and C_∞. Thus, it is difficult to quantitatively investigate the influence of changes in the temperature, humidity, and fiber content on the diffusion process. More important, because all existing studies have been based on the single-factor-analysis method, whether coupling effects among environmental factors exist is still not clear. Systematic experimental study and multifactor analysis are needed.

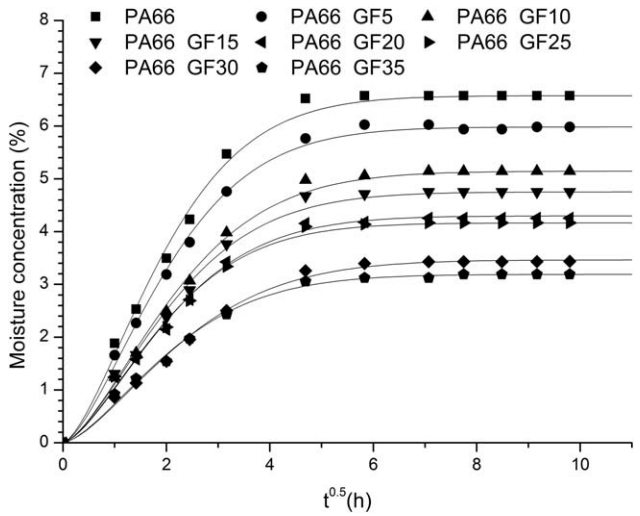

Figure 2. Weight gain curves of PA66 and its composites at 80°C and 95% RH.

Table I. Diffusion Parameters of PA66 and Its Composites

Material	C_∞ (%)	D (10^{-12} m^2/s)
PA66	6.5747	13.8806
PA66 GF5	5.9825	13.5031
PA66 GF10	5.1452	13.4793
PA66 GF15	4.7524	12.7618
PA66 GF20	4.2561	12.7131
PA66 GF25	4.1653	12.015
PA66 GF30	3.4648	10.9656
PA66 GF35	3.1908	10.6362

In this study, gravimetric experiments for neat and SGFR PA66s were carried out under different hydrothermal conditions. On the basis of thermodynamic and kinetic analysis, the influence of the fiber content, humidity, and temperature were investigated, and the underlying mechanism was expressed. In addition, the humidity–temperature coupling effect was investigated through analysis of variance, and the regression models were obtained.

EXPERIMENTAL

Materials and Sample Preparation

The PA66 used in this study was the commercially available Leona 1300S (Asahi Kasei Co., Ltd.), and the filled E-glass fiber density was 2.14×10^3 kg/m^3 (Nanjing Xingxing Co., Ltd.). The PA66 and glass fiber were premixed, and the mixture was stirred in a vessel until it was well blended. Then, it was directly fed into a SHJ-20 corotating double-screw extruder (Nanjing Giant Co., Ltd.) through an inlet. The desired composition was ensured by the weight ratio of fiber to polymer during mixing. The fiber contents were 5, 10, 15, 20, 25, 30, and 35 vol %, and the mixtures were labeled PA66 GF5 to PA66 GF35, respectively. The extruder was operated at a speed of 20 rpm, and the temperatures were 240°C at the feeding zone and 285°C at all of the other zones.

A sketch of the dumbbell-shaped specimens according to ASTM D 638 is depicted in Figure 1. The specimens were molded by a BS-III injection-molding machine (Borche Co., Ltd.). For the neat PA66 and its SGFR composites, the injection temperatures

Table II. C_∞ Values of Matrices of the Composites

Material	C_∞ (%)
PA66	6.5747
PA66 GF5	6.5612
PA66 GF10	6.1975
PA66 GF15	6.2971
PA66 GF20	6.2160
PA66 GF25	6.7225
PA66 GF30	6.1391
PA66 GF35	6.3561

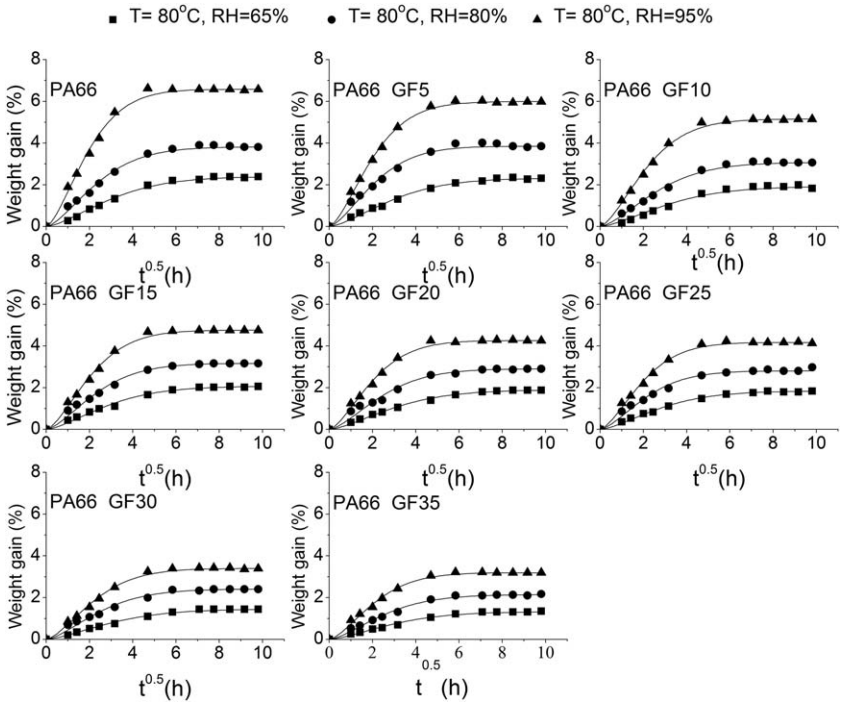

Figure 3. Weight gain curves of PA66 and its composites at 80°C and different RHs.

were 265 and 285°C, respectively. The mold was always kept at ambient temperature (20°C).

Gravimetrical Experiments

The specimens were preliminarily dried in a vacuum chamber until the weight was kept constant. Then, the dried specimens were placed in a KW-TH-80T temperature (T) and relative humidity (RH) test chamber (Kowin Co., Ltd.) under the following conditions: 40°C and 65% RH, 40°C and 95% RH, 60°C and 95% RH, 80°C and 65% RH, 80°C and 80% RH, and 80°C and 95% RH, respectively. They were wiped and weighed at intervals with an electronic analytical balance with a relative precision of 10^{-4}. The weighing was done at ambient temperature and required several minutes. Compared with the characteristic time of water diffusion (100 h), the weighing time was very short. Hence, the evaporated water during measurement was negligible. The moisture concentration (C_t) of each specimen was calculated in terms of its dried weight (w_o) and weight after exposure time t (w_t) as follows:

$$C_t(\%) = \frac{(w_t - w_o)}{w_o} \times 100\% \quad (2)$$

RESULTS AND DISCUSSION

Moisture diffusion processes in PA66 and its composites are generally studied against the square root of the exposure time which is labeled as $t^{0.5}$ in all following figure legends.[27] In this study, the moisture uptake curves of PA66 and its composites exposed at 80°C and 95% RH are depicted in Figure 2. Obviously, the diffusion processes in PA66 and its composites all obeyed the famous Fickian diffusion model.[14] Because the thickness of the samples was much smaller than their length and width, the diffusion process could be seen as one-dimensional, as described in eq. (1). For a plate of infinite dimensions, C_t can be represented as follows:

Table III. Parameters of Diffusion at 80°C and Different RHs

	C_∞ (%)			D (10^{-12} m^2/s)		
Material	65% RH	80% RH	95% RH	65% RH	80% RH	95% RH
PA66	2.3853	3.8073	6.5747	9.0456	9.4256	13.8806
PA66 GF5	2.3093	3.8427	5.9825	6.0056	8.2956	13.5031
PA66 GF10	1.9087	3.0641	5.1452	7.7425	8.0337	13.4793
PA66 GF15	2.0553	3.1620	4.7524	5.3012	6.8293	12.7618
PA66 GF20	1.8832	2.9001	4.2561	6.2843	6.4256	12.7131
PA66 GF25	1.8312	2.8007	4.1651	7.3250	7.5743	12.0150
PA66 GF30	1.4408	2.4054	3.3962	5.9981	6.2331	10.9656
PA66 GF35	1.3157	2.1381	3.1907	5.1637	6.6625	10.6362

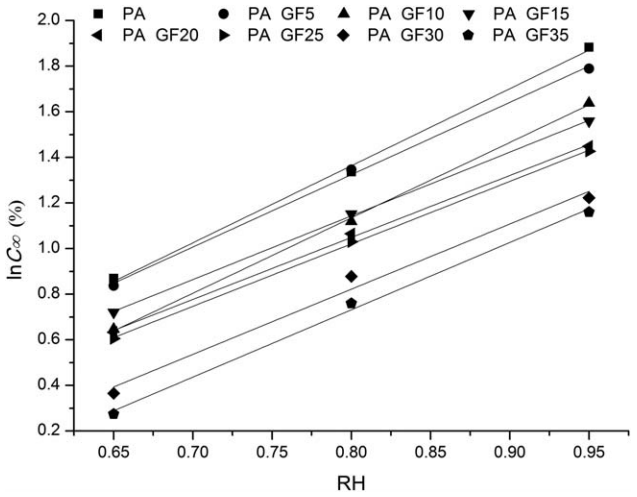

Figure 4. Fitted lines of ln C_∞ versus RH.

$$C_t = C_\infty \left\{ 1 - \frac{8}{\pi^2} \sum_{n=0}^{\infty} \frac{1}{(2n+1)^2} \exp\left[-\frac{Dt}{h^2} \pi^2 (2n+1)^2 \right] \right\} \quad (3)$$

where h is the thickness of the specimen, and n can be any arbitrary integer. Because of its complications, it is often approximated in a simple form as follows:

$$C_t = C_\infty \left\{ 1 - \exp\left[-7.3 \left(\frac{Dt}{h^2} \right)^{0.75} \right] \right\} \quad (4)$$

The value of C_∞ can be obtained directly from the gravimetric curve, such as the curves in Figure 2. With two points at t_1 and t_2 in the initial linear part of a gravimetric curve, D can determined with the following expression:[28]

Table IV. Parameters of the Natural Exponential Function

Material	a	b
PA66	0.2617	3.3797
PA66 GF5	0.2969	3.1729
PA66 GF10	0.2210	3.3055
PA66 GF15	0.3356	2.7941
PA66 GF20	0.3245	2.7179
PA66 GF25	0.3101	2.7392
PA66 GF30	0.2312	2.8582
PA66 GF35	0.1958	2.9528

$$D = \pi \left(\frac{h}{4C_\infty} \right)^2 \left(\frac{C_1 - C_2}{\sqrt{t_1} - \sqrt{t_2}} \right) \quad (5)$$

where C_1 and C_2 are are the moisture concentrations of the two points, respectively.

Influence of the Fiber Content

Figure 2 shows the water-uptake curves of PA66 and its seven composites with different levels of fiber loading. The corresponding parameters obtained through the aforementioned method are listed in Table I. D became gradually smaller as the fiber content increased. The main reason was that the incorporation of fibers extended the diffusion path length of water molecules in the composites. In addition, the fiber orientation along the thickness direction may also have affected the path length.

The C_∞ values of the composites decreased with the addition of fiber content. However, as water was absorbed by the matrices of composites, the C_∞ values of the matrices were recalculated and are presented in Table II. There was no obvious trend in

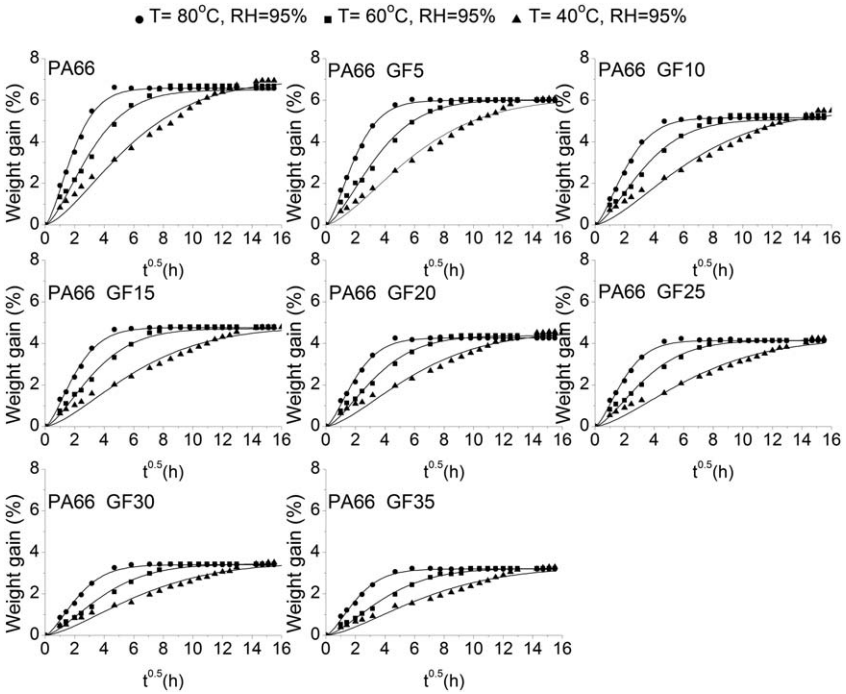

Figure 5. Weight gain curves of PA66 and its composites at 95% RH and different temperatures.

Table V. Parameters of Diffusion at 95% RH and Different Temperatures

	C_∞ (%)			D (10^{-12} m^2/s)		
Material	40°C	60°C	80°C	40°C	60°C	80°C
PA66	6.9425	6.6827	6.5747	1.2681	4.2443	13.8806
PA66 GF5	6.0825	6.0205	5.9825	1.1212	3.6737	13.5031
PA66 GF10	5.4885	5.2622	5.1452	1.1062	3.9262	13.4793
PA66 GF15	4.8826	4.7935	4.7524	1.1381	4.5287	12.7618
PA66 GF20	4.5574	4.3691	4.2561	1.1006	4.0225	12.7131
PA66 GF25	4.2426	4.1433	4.1292	1.0581	3.8906	12.0150
PA66 GF30	3.5051	3.4364	3.3962	1.0356	3.6587	10.9656
PA66 GF35	3.2870	3.2236	3.1907	0.9637	3.1968	10.6362

which the equilibrium contents in the matrices of the composites varied with the fiber content. The maximum percentage deviation from the neat PA66 was less than 7% (6.1391–6.5747%). The differences may have been due to the interface of the fiber and the matrix. If voids existed in the interfaces, the water uptake would have increased. When bonding at the interface was good, it may have inhibited water uptake. Hence, the fiber content almost had no effect on the C_∞ values of the matrices.

Influence of RH

Weight-gain fitted curves of PA66 and its composites with different RHs are presented in Figure 3. From the curves and method described in eq. (5), the parameters of moisture uptake were obtained and are displayed in Table III. Obviously, the velocity of diffusion was faster with higher RH. At lower RH, only a limited number of water molecules were in the active state. At higher RH, the quantity of active molecules increased. In addition, when the moisture content of the PA66 reached a level at which the glass-transition temperature dropped, it offered more active sites for sorption due to plasticization.[29] Hence, a high RH led to a high velocity of diffusion.

The values of C_∞ became larger with RH. The diffusion process achieved its equilibrium state when the chemical potentials of water molecules in moisture and the composites were equal. With the assumption of the atmosphere as an ideal gas, the chemical potentials of water under an ambient environment can be calculated with Raoult's law:

$$\mu_i^{(l)} = \mu_i^*(T,p) + RT\ln \text{ RH} \tag{6}$$

where $\mu_i^{(l)}$ is the chemical potential of water under an ambient environment, $\mu_i^*(T,p)$ is the chemical potential of pure water vapor and R is the gas constant (8.314 J K^{-1} mol^{-1}). The chemical potential of water molecules in the composites is described as follows:

$$\mu_i^{(w)} = \mu_i^*(T,p) + RT\ln(\gamma N) \tag{7}$$

where $\mu_i^{(w)}$ is the chemical potential of water molecules in the composites, γ is the fugacity coefficient and N is the molar fraction of water in the PA66 and composites. When γ is equal to 1, the solution is an ideal solution. N is proportional to the concentration (C) as follows:

$$C = \alpha N \quad (\alpha > 0) \tag{8}$$

where α is a proportionality coefficient. With eqs. (6–8), the following equation can be derived:

$$C_\infty = \frac{RH}{\alpha\gamma} \tag{9}$$

In the ideal state, C_∞ is proportional to RH. There are some deviations under practical situations. However, the positive correlation

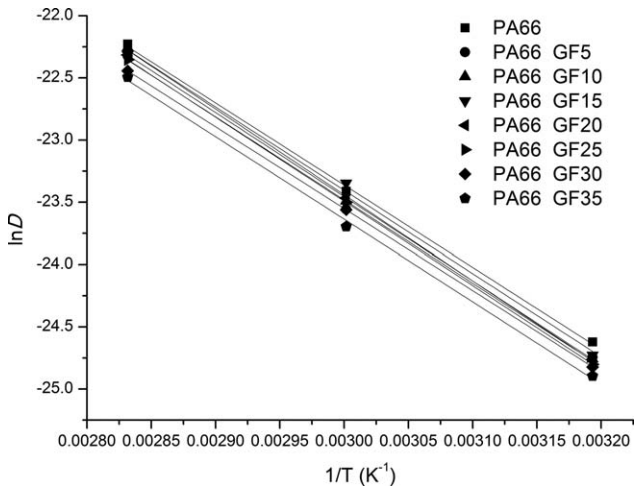

Figure 6. Fitted lines of ln D versus $1/T$.

Table VI. Values of Activation Energy

Material	Q (kJ/mol)
PA66	6.6089
PA66 GF5	6.6841
PA66 GF10	6.9059
PA66 GF15	6.6933
PA66 GF20	6.7633
PA66 GF25	6.7655
PA66 GF30	6.5798
PA66 GF35	6.6300

Table VII. Enthalpy Changes (ΔH)of the Water Uptake in PA66 and Its Composites

Material	ΔH (kJ/mol)
PA66	−1.2598
PA66 GF5	−0.3824
PA66 GF10	−1.4920
PA66 GF15	−0.6251
PA66 GF20	−1.5778
PA66 GF25	−0.6313
PA66 GF30	−0.7283
PA66 GF35	−0.6869

trend will still exist. With the phenomenological method and experiment data analysis, the following model was proposed:

$$C_\infty(\%) = ae^{bRH} \tag{10}$$

where a and b are the corresponding parameters. The corresponding fitted lines of ln C_∞ versus RH are plotted in Figure 4. Because the coefficients of determination for all of the fitted lines were more than 0.99, a natural exponential function to the model relation between C_∞ and RH was credible. The parameters of eq. (10) are given in Table IV.

Influence of the Temperature

Diffusion is known as a thermally activated process, and temperature usually plays a very important role in the diffusion of molecules.[19] Figure 5 shows the weight gain curves of the PA66 and composites under different temperatures. The parameters of the Fickian model calculated by the aforementioned method are listed in Table V.

The diffusion velocity, similar to the reaction rates, usually follows the Arrhenius law:[19]

$$D = D_o e^{-Q/RT} \tag{11}$$

where Q is the activation energy and is assumed to not depend on the temperature in a limited temperature range. D_o is a constant. As shown in Figure 6, ln D decreases with $1/T$, and separated data points can be fitted well to straight lines. Therefore, D also obeys the Arrhenius law. The activity energies obtained from the slopes of the lines are presented in Table VI. The results illustrate that the activation energies fluctuated in a small range with fiber content variation, and the maximum relative deviation was 4.95%.

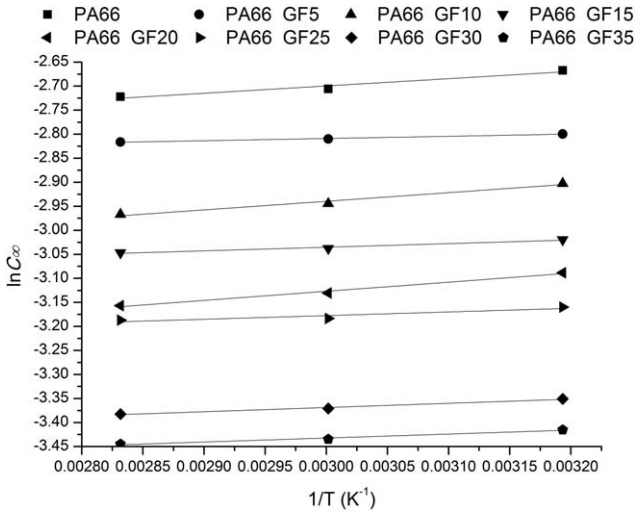

Figure 7. Fitted lines of ln C_∞ versus $1/T$.

According to van't Hoff's equation, the temperature-dependent C_∞ of the solute can be determined by the enthalpy change upon solution[2,30] as follows

$$\frac{d\ln C_\infty}{dT} = -\frac{\Delta H(T)}{RT^2} \tag{12}$$

where $\Delta H(T)$ is the mixing enthalpy change between PA66 and water. PA66 and its composites with water uptake could be regarded as dilute solutions and were expected to follow van't Hoff's equation. In the temperature range of measurement, $\Delta H(T)$ could be regarded as a constant. Hence, the integration of eq. (12) leads to

$$C_\infty = C_o \exp\left(\frac{-\Delta H}{RT}\right) \tag{13}$$

where C_o is a constant pre-exponential factor. The variation of ln C_∞ with $1/T$ is shown in Figure 7. Obviously, linear relations

Table VIII. Tests of Between-Subjects Effects for the C_∞

Source	Type III sum of squares	*df*	Mean square	*F*	Significance
Corrected model	310.499[a]	10	31.050	168.285	0.000
Intercept	1444.326	1	1444.326	7827.982	0.000
Composites	89.223	7	12.746	69.082	0.000
Temperature	70.251	1	70.251	380.745	0.000
Humidity	70.251	1	70.251	380.745	0.000
Temperature × humidity	80.774	1	80.774	437.782	0.000
Error	15.683	85	0.185		
Total	1770.508	96			
Corrected total	326.182	95			

[a] $R^2 = 0.952$ (adjusted $R^2 = 0.946$). *df*: degree of freedom.

Table IX. Tests of Between-Subjects Effects for D

Source	Type III sum of squares	*df*	Mean square	*F*	Significance
Corrected model	2042.828[a]	10	204.283	281.413	0.000
Intercept	2481.553	1	2481.553	3418.502	0.000
Composites	24.315	7	3.474	4.785	0.000
Temperature	1439.634	1	1439.634	1983.190	0.000
Humidity	255.310	1	255.310	351.706	0.000
Temperature × Humidity	323.570	1	323.570	445.739	0.000
Error	61.703	85	0.726		
Total	4586.084	96			
Corrected total	2104.531	95			

[a] $R^2 = 0.971$ (adjusted $R^2 = 0.946$). *df*: degree of freedom.

Table X. Model Summary for C_∞

Model	*R*	R^2	Adjusted R^2	Standard error of estimate
1	0.871[a]	0.758	0.755	0.904634939
2	0.959[b]	0.919	0.918	0.524765906
3	0.961[c]	0.924	0.922	0.511298226
4	0.967[d]	0.935	0.932	0.475924882

[a] Predictive variables: constant and RH.
[b] Predictive variables: constant, RH, and *F*.
[c] Predictive variables: constant, RH, *F*, and *T*.
[d] Predictive variables: constant, RH, *F*, *T*, and RH × *T*.

could be established, and this was consistent with van't Hoff's equation. The enthalpy changes could be obtained from the slopes of the fitted lines in Figure 7 and are exhibited in Table VII. The negative values of enthalpy changes manifested that the moisture diffusion in PA66 and its composites was a slightly exothermic process.

Consequently, C_∞ was expected to decrease with increasing temperature. However, the values of ΔH for the PA66 and composites were rather small, and the maximum relative deviation of C_∞ was 7.08% within the narrow temperature range of this study. Thus, C_∞ only weakly depended on the temperature. Similar results were found in the studies in refs. 19 and 30.

Humidity–Temperature Coupling Effect

From previous analysis, the effects of the humidity and temperature on moisture diffusion were studied independently through single-factor analysis without interaction. Through multifactor analysis of variance, the coupling effect between the humidity and temperature was studied.

From experiments and analysis, the calculated diffusion parameters of polyamide (PA) and its composites are listed in Appendix A under different hydrothermal conditions. After analysis with the software IBM SPSS Statistics 19.0, the results are listed in Tables VIII and IX. For a factor, if the value of significance is less than 0.01, its influence is significant. The data implies that

Table XI. Analysis of Variance for C_∞

Model		Sum of squares	*df*	Mean square	*F*	Significance
1	Regression	240.699	1	240.699	294.122	0.000[a]
	Residual	76.926	94	0.818		
	Total	317.625	95			
2	Regression	292.015	2	146.008	530.205	0.000[b]
	Residual	25.610	93	0.275		
	Total	317.625	95			
3	Regression	293.574	3	97.858	374.324	0.000[c]
	Residual	24.051	92	0.261		
	Total	317.625	95			
4	Regression	297.013	4	74.253	327.823	0.000[d]
	Residual	20.612	91	0.227		
	Total	317.625	95			

[a] Predictive variables: constant and RH.
[b] Predictive variables: constant, RH, and *F*.
[c] Predictive variables: constant, RH, *F*, and *T*.
[d] Predictive variables: constant, RH, *F*, *T*, and RH × *T*. *df*: degree of freedom.

Table XII. Coefficients of Regression Equations of C_∞

Model		Unstandardized coefficients		Standardized coefficients		
		B	Standard error	*β*	*t*	Significance
1	Constant	−5.294	0.501		−10.567	0.000
	RH	10.556	0.616	0.871	17.150	0.000
2	Constant	−4.177	0.302		−13.836	0.000
	RH	10.556	0.357	0.871	29.565	0.000
	F	−6.382	0.467	−0.402	−13.651	0.000
3	Constant	−4.560	0.333		−13.683	0.000
	RH	10.556	0.348	0.871	30.343	0.000
	F	−6.382	0.456	−0.402	−14.010	0.000
	T	.006	0.003	0.070	2.442	0.017
4	Constant	−7.588	0.837		−9.068	0.000
	RH	14.342	1.024	1.183	14.005	0.000
	F	−6.382	0.424	−0.402	−15.052	0.000
	T	0.057	0.013	0.625	4.313	0.000
	RH × *T*	−0.063	0.016	−0.645	−3.897	0.000

B: regression coefficient
β: standardized regression coefficient.

Table XIII. Model Summary for *D*

Model	*R*	R^2	Adjusted R^2	Standard error of estimate
1	0.943[a]	0.890	0.888	1.572118582
2	0.951[b]	0.905	0.903	1.467363258
3	0.979[c]	0.959	0.958	0.966944028
4	0.982[d]	0.965	0.963	0.899482242

[a] Predictive variables: constant and RH × *T*.
[b] Predictive variables: constant, RH × *T*, and RH × RH.
[c] Predictive variables: constant, RH × *T*, RH × RH, and *T* × *T*.
[d] Predictive variables: constant, RH × *T*, RH × RH, *T* × *T*, and *F* × *F*.

the humidity–temperature coupling effects for C_∞ and *D* both are significant.

To precisely represent the influences of the aforementioned factors on *D* and C_∞, nonlinear multiple regression models were obtained by the quadratic polynomial stepwise regression method. In this method, according to the influence degree of all possible independent variables to dependent variables, from large to small, the factors were successively introduced to the regression equations one by one.

Tables X and XI exhibit the results for C_∞, where *F* denotes the fiber content. The data demonstrates that the effect levels of these factors on C_∞ were successively the RH, fiber content,

Table XIV. Analysis of Variance for *D*

Model		Sum of squares	*df*	Mean square	*F*	Significance
1	Regression	1872.205	1	1872.205	757.500	0.000[a]
	Residual	232.326	94	2.472		
	Total	2104.531	95			
2	Regression	1904.288	2	952.144	442.209	0.000[b]
	Residual	200.243	93	2.153		
	Total	2104.531	95			
3	Regression	2018.513	3	672.838	719.627	0.000[c]
	Residual	86.018	92	0.935		
	Total	2104.531	95			
4	Regression	2030.906	4	507.726	627.545	0.000[d]
	Residual	73.625	91	0.809		
	Total	2104.531	95			

[a] Predictive variables: constant and RH × *T*.
[b] Predictive variables: constant, RH × *T*, and RH × RH.
[c] Predictive variables: constant, RH × *T*, RH × RH, and *T* × *T*.
[d] Predictive variables: constant, RH × *T*, RH × RH, *T* × *T*, and *F* × *F*. *df*: degree of freedom.

Table XV. Coefficients of Regression Equations of D

Model		Unstandardized coefficients		Standardized coefficients		
		B	Standard error	β	t	Significance
1	Constant	−6.312	0.444		−14.213	0.000
	RH × T	0.237	0.009	0.943	27.523	0.000
2	Constant	−5.313	0.489		−10.874	0.000
	RH × T	0.255	0.009	1.011	27.674	0.000
	RH × RH	−2.752	0.713	−0.141	−3.860	0.000
3	Constant	−3.723	0.353		−10.559	0.000
	RH × T	0.612	0.033	2.431	18.603	0.000
	RH × RH	−16.154	1.300	−0.828	−12.423	0.000
	T × T	−0.002	0.000	−1.264	−11.053	0.000
4	Constant	−3.346	0.342		−9.788	0.000
	RH × T	0.612	0.031	2.431	19.998	0.000
	RH × RH	−16.154	1.210	−0.828	−13.355	0.000
	T × T	−0.002	0.000	−1.264	−11.882	0.000
	F × F	−8.616	2.201	−0.077	−3.914	0.000

B: regression coefficient
β: standardized regression coefficient.

temperature, and interaction between the humidity and temperature. The optimal regression equation of C_∞ (%) is as follows:

$$C_\infty(\%) = -7.588 + 14.342\text{RH} - 6.382F + 0.057T - 0.063\text{RH} \times T \quad (14)$$

As shown in Tables (XIII–XV), the positive coupling effect is the main factor influencing the diffusion velocity. Among optional models, the optimal one is as follows:

$$D(10^{-2}) = -3.346 + 0.612\text{RH} \times T - 16.154\text{RH} \times \text{RH} - 0.002T \times T - 8.616F \times F \quad (15)$$

The two regression equations manifest that the humidity–temperature coupling effect plays an important role in the moisture diffusion process, especially for diffusion velocity.

CONCLUSIONS

In this study, the moisture diffusion in PA66 and its short fiber-reinforced composites was investigated by a gravimetric experiment. The following conclusions were drawn:

1. The equilibrium moisture concentration in a SGFR PA66 decreased as the fiber content increased. However, the existence of the fiber worked as barrier to decrease the diffusion velocity.
2. C_∞ only weakly depended on the temperature because moisture diffusion is a very slight exothermal process. As diffusion is a thermally activated process, it accelerated at a higher temperature.
3. The high level of RH increased both the equilibrium moisture concentration and diffusion velocity. A proposed natural exponential function was proposed to model well the relation between the equilibrium moisture concentration and RH.
4. The humidity–temperature coupling effect played an important role in the moisture diffusion process. It was the largest factor for diffusion velocity. For C_∞, its influence was lower than those of humidity, fiber content, and temperature.

ACKNOWLEDGMENTS

The authors acknowledge the financial support of the National Natural Science Foundation Council of China (contract grant numbers 51125021 and 51210004) and the National Program on Key Basic Research Project (contract grant numbers 2012CB025903 and 2013CB035805).

Appendix A. Data for the Analysis of Variance

Materials	Fiber loading (vol %)	Temperature (°C)	Humidity (RH; %)	Diffusion coefficient (10^{-12})	Equilibrium concentration (%)
PA66	0	40	65	1.4807	1.8391
PA66	0	40	65	1.4807	1.8391
PA66	0	40	65	1.3095	1.8391
PA66 GF5	5	40	65	1.8462	1.3072
PA66 GF5	5	40	65	1.4291	1.5251
PA66 GF5	5	40	65	1.4291	1.5251

Appendix A. *Continued*

Materials	Fiber loading (vol %)	Temperature (°C)	Humidity (RH; %)	Diffusion coefficient (10^{-12})	Equilibrium concentration (%)
PA66 GF10	10	40	65	1.1305	1.4553
PA66 GF10	10	40	65	1.4292	1.4553
PA66 GF10	10	40	65	1.5072	1.2474
PA66 GF15	15	40	65	1.5071	1.1881
PA66 GF15	15	40	65	1.4292	1.3861
PA66 GF15	15	40	65	0.9043	1.3861
PA66 GF20	20	40	65	1.2308	1.1299
PA66 GF20	20	40	65	1.1074	1.3183
PA66 GF20	20	40	65	0.9043	1.3183
PA66 GF25	25	40	65	2.1702	0.8945
PA66 GF25	25	40	65	1.2308	1.0733
PA66 GF25	25	40	65	1.2308	1.0733
PA66 GF30	30	40	65	2.1703	0.8576
PA66 GF30	30	40	65	1.2308	1.0292
PA66 GF30	30	40	65	1.2308	1.0292
PA66 GF35	35	40	65	1.7491	0.6568
PA66 GF35	35	40	65	1.7723	0.8210
PA66 GF35	35	40	65	1.0944	0.8210
PA66	0	40	95	1.0934	6.8966
PA66	0	40	95	1.1144	6.8966
PA66	0	40	95	1.0499	7.1264
PA66 GF5	5	40	95	0.9922	5.8952
PA66 GF5	5	40	95	1.0144	5.8952
PA66 GF5	5	40	95	0.9063	6.1135
PA66 GF10	10	40	95	1.0267	5.4054
PA66 GF10	10	40	95	1.0623	5.4054
PA66 GF10	10	40	95	0.9739	5.6133
PA66 GF15	15	40	95	1.0155	4.7431
PA66 GF15	15	40	95	1.0595	4.7431
PA66 GF15	15	40	95	0.9732	4.9407
PA66 GF20	20	40	95	1.0414	4.5198
PA66 GF20	20	40	95	1.1147	4.5198
PA66 GF20	20	40	95	1.0164	4.7081
PA66 GF25	25	40	95	0.9344	3.9427
PA66 GF25	25	40	95	1.0195	3.9426
PA66 GF25	25	40	95	0.9328	4.12187
PA66 GF30	30	40	95	1.0555	3.4364
PA66 GF30	30	40	95	0.9819	3.4364
PA66 GF30	30	40	95	0.9260	3.6082
PA66 GF35	35	40	95	0.9988	2.9557
PA66 GF35	35	40	95	0.9318	3.1199
PA66 GF35	35	40	95	0.9243	3.1199
PA66	0	80	65	6.9369	2.2936
PA66	0	80	65	7.8228	2.2936
PA66	0	80	65	5.2587	2.5229
PA66 GF5	5	80	65	5.4432	2.1786
PA66 GF5	5	80	65	3.7189	2.3965

Appendix A. *Continued*

Materials	Fiber loading (vol %)	Temperature (°C)	Humidity (RH; %)	Diffusion coefficient (10^{-12})	Equilibrium concentration (%)
PA66 GF5	5	80	65	5.6627	2.3965
PA66 GF10	10	80	65	9.5623	1.6598
PA66 GF10	10	80	65	7.5554	1.8672
PA66 GF10	10	80	65	7.7775	1.8672
PA66 GF15	15	80	65	5.1785	1.9763
PA66 GF15	15	80	65	5.6557	1.9763
PA66 GF15	15	80	65	3.6750	2.1739
PA66 GF20	20	80	65	5.7462	1.6949
PA66 GF20	20	80	65	4.1315	1.8832
PA66 GF20	20	80	65	3.7190	2.0716
PA66 GF25	25	80	65	5.2359	1.7953
PA66 GF25	25	80	65	4.6544	1.7953
PA66 GF25	25	80	65	4.4504	1.9749
PA66 GF30	30	80	65	4.8573	1.3722
PA66 GF30	30	80	65	6.1068	1.3722
PA66 GF30	30	80	65	4.7677	1.5437
PA66 GF35	35	80	65	4.8577	1.3158
PA66 GF35	35	80	65	4.2187	1.3157
PA66 GF35	35	80	65	4.7679	1.4803
PA66	0	80	95	13.1887	6.4368
PA66	0	80	95	13.0038	6.6667
PA66	0	80	95	12.9411	6.6667
PA66 GF5	5	80	95	13.3362	5.6768
PA66 GF5	5	80	95	13.1311	5.8952
PA66 GF5	5	80	95	11.1767	6.3319
PA66 GF10	10	80	95	14.4241	4.9792
PA66 GF10	10	80	95	13.2497	5.1867
PA66 GF10	10	80	95	14.2319	5.1867
PA66 GF15	15	80	95	12.9956	4.7525
PA66 GF15	15	80	95	13.1563	4.7525
PA66 GF15	15	80	95	12.3707	4.7525
PA66 GF20	20	80	95	13.4114	4.1431
PA66 GF20	20	80	95	12.2393	4.3314
PA66 GF20	20	80	95	12.2706	4.3315
PA66 GF25	25	80	95	12.2629	3.9497
PA66 GF25	25	80	95	12.4662	3.9497
PA66 GF25	25	80	95	12.1536	4.4883
PA66 GF30	30	80	95	12.4874	3.2590
PA66 GF30	30	80	95	11.0917	3.4305
PA66 GF30	30	80	95	11.0418	3.4305
PA66 GF35	35	80	95	11.4717	3.1250
PA66 GF35	35	80	95	11.0980	3.1250
PA66 GF35	35	80	95	8.9615	3.2895

REFERENCES

1. Hassan, A.; Salleh, N. M.; Yahya, R.; Sheikh, M. J. *Reinf. Plast. Compos.* **2011**, *30*, 488.
2. Bao, L.-R.; Yee, A. F. *Polymer* **2002**, *43*, 3987.
3. El Mazry, C.; Correc, O.; Colin, X. In International Conference on Times of Polymers (TOP) and Composites Conference Proceedings; AIP: Ischia, Italy, **2010**; p 135.
4. Launay, A.; Marco, Y.; Maitournam, M.; Raoult, I. *Mech. Mater.* **2013**, *56*, 1.
5. Miri, V.; Persyn, O.; Lefebvre, J.-M.; Seguela, R. *Eur. Polym. J.* **2009**, *45*, 757.
6. Hassan, A.; Rahman, N. A.; Yahya, R. *Fiber Polym.* **2012**, *13*, 899.
7. Thomason, J. L.; Porteus, G. *Polym. Compos.* **2011**, *32*, 639.
8. Flory, P. J. J. *Chem. Phys.* **1942**, *10*, 51.
9. Huggins, M. L. Ann, N. Y. *Acad. Sci.* **1942**, *43*, 1.
10. Favre, E.; Nguyen, Q.; Clément, R.; Néel, J. *J. Membr. Sci.* **1996**, *117*, 227.
11. Park, G. S. Synthetic Membranes: Science, Engineering and Applications; Springer: New York, **1986**; p 57.
12. Guggenheim, E. A. Applications of Statistical Mechanics; Oxford University Press: Oxford, **1966**.
13. De Boer, J. The Dynamic Character of Adsorption; Oxford University Press: Clarendon, England, **1953**.
14. Crank, J. The Mathematics of Diffusion; Oxford University Press: Oxford, **1979**.
15. Yu, Y. T.; Pochiraju, K. *Polym. Plast. Technol.* **2003**, *42*, 737.
16. Grace, L.; Altan, M. *Compos. A* **2012**, *43*, 1187.
17. Post, N.; Riebel, F.; Zhou, A.; Keller, T.; Case, S.; Lesko, J. *J. Compos. Mater.* **2008**, *43*, 75.
18. Kelly, A.; Zweben, C. H. Comprehensive Composite Materials; Elsevier: Amsterdam, **2000**.
19. Abacha, N.; Kubouchi, M.; Sakai, T. *Express Polym. Lett.* **2009**, *3*, 245.
20. McKague, E.; Halkias, J.; Reynolds, J. *J. Compos. Mater.* **1975**, *9*, 2.
21. Chateauminois, A.; Vincent, L.; Chabert, B.; Soulier, J. *Polymer* **1994**, *35*, 4766.
22. Chaplin, A.; Hamerton, I.; Herman, H.; Mudhar, A.; Shaw, S. *Polymer* **2000**, *41*, 3945.
23. El-Sa'ad, L.; Darby, M.; Yates, B. *J. Mater. Sci.* **1990**, *25*, 3577.
24. Mohd Ishak, Z.; Ariffin, A.; Senawi, R. *Eur. Polym. J.* **2001**, *37*, 1635.
25. Jiang, X.; Kolstein, H.; Bijlaard, F. S. *Compos. B* **2013**, *45*, 407.
26. Joannès, S.; Mazé, L.; Bunsell, A. R. *Compos. Struct.* **2014**, *108*, 111.
27. Thomason, J.; Ali, J.; Anderson, J. *Compos. A* **2010**, *41*, 820.
28. Jiang, X.; Kolstein, H.; Bijlaard, F. S. *Mater. Design.* **2012**, *37*, 304.
29. Lim, L. T.; Britt, I. J.; Tung, M. A. *J. Appl. Polym. Sci.* **1999**, *71*, 197.
30. Wang, J.; Li, K.-X.; He, H.-W.; Wang, J.-L.; Sun, G.-H. *Colloid Surf. A.* **2011**, *377*, 330.